

HEAT and DUST TRANSPORT IN A PEBBLE BED HTR

Jayaraju S.T.* , Shams A., and Roelofs F.

Nuclear Research & Consultancy Group
Westerduinweg 3, 1755ZG, Petten, The Netherlands
Jayaraju@nrg.eu

ABSTRACT

The flow behavior in pebble bed reactors is typically analyzed using lumped parameter or porous medium approaches. Such approaches inhibit averaging of flow quantities over large volumes. The ever increasing computational power and advanced numerical CFD methods allow a more detailed assessment of the flow behavior, and especially the heat and dust transport in a pebble bed.

The first part of this paper discusses Large Eddy Simulation results of the flow and heat transport in a randomly stacked bed of spherical pebbles, using a second-order accurate, cell-centered finite volume method on an unstructured polyhedral mesh. The predicted flow-field is fairly complex and exhibits highly unsteady and three-dimensional turbulent behavior with strong rotational and cross flow regions. The reported analyses results can be used for validation of low-order turbulence modeling applications to complex pebble flow configurations.

While Large Eddy Simulation is a more accurate methodology to study the flow and heat transport, it becomes impractical to use it for dust transport studies due to large computational costs in tracking several thousands of dust particles individually. Owing to this limitation, the second part of this paper focusses on Reynolds Averaged Navier Stokes modeling of flow and dust transport in a random pebble bed arrangement. The dust transport model used in the present study is validated across two test cases of flow over single and array of spheres where reference experimental data are available. Finally, this validated model is used to analyze the dust transport and deposition patterns in a randomly stacked pebble-bed arrangement.

KEYWORDS

Heat transport, dust transport, pebble bed, HTR, LES, RANS

1. INTRODUCTION

An HTR uses helium gas as a coolant, while the moderator function is performed by carbon in the form of graphite [1]. The fuel is embedded in the graphite moderator and can withstand very high temperatures [2-3], as an important safety feature of HTRs, basically preventing the fuel from melting. Various experimental pebble bed reactors have successfully been operated worldwide [4]. They have shown safe and efficient operation, however questions have been raised regarding the potential occurrence of local hot-spots in the pebble bed, possibly affecting the pebble integrity [5]. Heat transfer around spherical surface varies noticeably for both laminar and turbulent flow regimes and the obvious appearance of the curved flow. The flow passages through the gaps between the pebbles could have concave and convex configurations, and the manifestation of centrifugal forces comes into play in the form of suppression or augmentation of turbulence level [6]. In addition, pressure gradients strongly affect the boundary layers. Transition from laminar to turbulent, wake, flow separation and its respective reattachment make this

* Corresponding Author

flow configuration very complex. Therefore, a detailed evaluation of a pebble bed flow physics is needed. The first part of this article deals with the flow and heat transport analysis for a randomly stacked, spherical shape, pebble bed at a moderate Reynolds number by using high fidelity LES approach.

The pebbles are primarily made of graphite and contain uranium dispersed in coated sand-size grains throughout the pebble. One of the sources of dust production is due to the abrasion of randomly stacked graphite pebbles. The generated dust is essentially composed of carbonaceous compounds, fission and activation products. In the AVR operations between 1967-1988, abraded dust is anticipated to be in the range of 60 kg/yr. The dust is eventually carried by helium gas through the primary circuit and gets deposited in its main components such as the main pipes systems, the heat exchangers and turbo-machinery. Deposition and remobilization of dust deposited in the primary system is identified as one of the foremost concerns during a depressurization accident [7]. Hence, accurate prediction of dust transport and deposition is an important step in the design of this type of reactors. The second part of this article deals with the dust transport and deposition modeling in a randomly stacked pebble bed using the most commonly used RANS methodology.

2. VALIDATION APPROACH

2.1. Flow & Heat Transport

Complex flow fields, encountered in many engineering applications, are highly three-dimensional, unsteady, separated and turbulent in nature. One such example is a characterization of flow and heat transport in a pebble bed configuration. In this regard, a number of experimental studies have been made to understand such a complex flow physics, a few example are [8-10]. Although, the experimental measurements provide a good qualitative picture of the flow and heat transport phenomena, however, the provided information is not sufficient enough to validate the low order CFD approaches, such as RANS modelling. Main limitations in the available experimental data lie in the exact replication of boundary conditions and/or exact position of the pebbles. On the other hands, high quality CFD could play an important role in order to fill this gap by providing a reference database. In term of quality, DNS is regarded as a numerical experiment, however, its applicability for a complex pebble bed distribution, e.g. randomly stacked configuration, is extremely difficult. In such scenarios, Large eddy simulations (LES) have played an important role in filling the existing gap, for high fidelity numerical solution [11-12]. The significantly reduced computational effort, in comparison to Direct Numerical Simulation (DNS), has made this CFD technique attractive for a growing range of industrial applications. Simulations involving flow over complex geometries have already been attempted using unstructured grid techniques. Moreover, several attempts have been made to show the ability of unstructured methods to accurately simulate flows involving large-scale unsteadiness. The appeal of accurately solving complex real life problems, by means of the efficient cell or element distribution offered by unstructured grids, motivates continued research in this area. Several flow examples for simple geometries, which expose the challenge of simulating complex separated turbulent flows, are also widely adopted in the literature to support the fundamental development of turbulence models and numerical methods. Representative databases available in literature include for example, flow over a backward-facing step, flow around a square prism, flow over a cube, and other bluff bodies such as a circular cylinder, sphere, and spheroid etc. Such simplified flow configuration are considered representative of specific flow phenomena developing in realistic complex 3D engineering geometries. The scope of the first part of this article is to extend the range of available fundamental databases by delivering reference results for flow in complex pebble bed configurations, which can be used to develop and validate lower order Reynolds Averaged Navier Stokes (RANS) closures.

2.2. Dust Transport

CFD modeling has emerged as a useful tool in simulating the particle transport and deposition phenomena. While DNS and LES are the advanced modeling methodologies which result in realistic particle deposition predictions, tracking several hundred thousands of particles with the refinement levels of DNS/LES is computationally very expensive even for a limited size pebble bed. The widely used RANS methodology is the most practical approach to consider. Within the RANS approach, it is generally seen that accounting for near wall anisotropy is important to predict accurate particle deposition in wall bounded flows [13]. Most of the recent literature on particle deposition using RANS modeling of wall bounded flows focusses on accurate modeling of the near-wall anisotropy. In our recent study [14], several uncertainties regarding the near-wall modeling and the turbulence modeling were addressed. The main outcome of this study was a carefully chosen RANS model coupled with a specific near-wall correlation for reliable particle transport and deposition prediction in duct flows. The objective of the second part of the present article is to apply the proposed model in [14] to the validation cases of flow over single and array of spheres where reference experimental data are available. Finally, this validated model is used to analyze the particle transport and deposition patterns in a randomly stacked pebble-bed arrangement.

3. CFD ASPECTS

3.1. Computational Domain

3.1.1. Flow and heat transport



Figure 1. Schematic of the computational domain (left) iso-metric view (right) top view.

The selected flow domain is a randomly stacked bed of spherical shape pebbles in a rectangular domain of $x=0.177$ m, $y=0.354$ and $z=0.177$ m, shown in Fig. 1. This flow domain is representative of the core of an HTR. This random pebble geometry is obtained from the work of [15], consists of 30 pebbles, and exhibits an average porosity (ϵ =volume of voids/total volume) level of 0.4. The diameter of the pebbles is 6 cm, consistent with the specification of PMBR-250MWth [9-10]. All pebbles are clustered in a cubic domain of 0.177 m per side, while the requirement for inlet and outlet boundary conditions leads to the extension of the computational domain in the y-direction, i.e. 0.0885 m for both inlet and outlet sections. Modeling the contact area between the pebbles also requires particular attention. Straightforward geometrical representation would consider a point contact between pebbles. However, modeling such point contacts is problematic from a meshing view point, which may induce numerical errors to the solution, and may also not be representative of realistic reactor cores, where the weight of the pebble bed probably leads to small area contacts. Therefore, small area contacts are modeled in the simulations, and are obtained by scaling the pebbles by a factor of 1.034. This makes the porosity slightly less than 0.4.

3.1.2. Dust transport

As mentioned in the validation approach, the dust transport model for anisotropic particle tracking using RANS approach [14] is first validated on two validation cases of flow over single sphere and flow over array of spheres respectively. This validated model is finally used for analyzing particle deposition patterns in a random pebble-bed arrangement.

The computational domains for the single sphere and the array of spheres as shown in Fig. 2 are based on the experiments of [16]. The spheres have a diameter of 6.5 mm. In both cases, only one fourth of the domain is modeled due to symmetry reasons. The computational domain starts seven sphere diameters upstream to allow developed conditions for flow and particles. The domain is extended seven sphere diameters downstream to ensure no influence of recirculation zone behind the last sphere on the particle deposition.

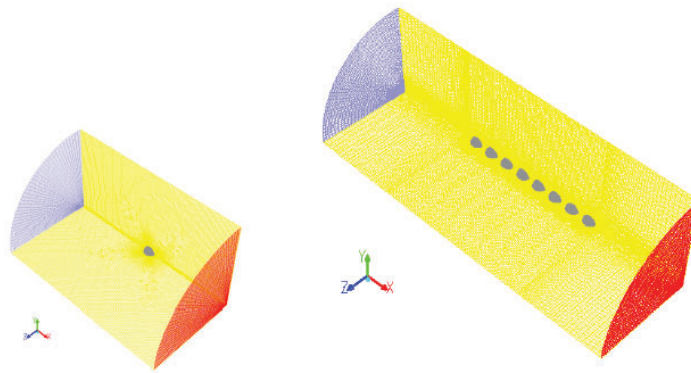


Figure 2. Schematic of the computational domain for (left) flow over single sphere and (right) array of spheres.

The next part of the dust transport study is on the randomly stacked pebble-beds. The considered randomly stacked pebble-bed geometry is similar to the one where flow and heat transport are studied, however, in order to avoid area contacts altogether, a scaling down is performed on the random arrangement. A small scaling-down factor of 0.966 is applied to achieve no point/area contacts. This results in an over-all porosity which is slightly higher than 0.4. The domain is extended, both on the inlet and the outlet side to avoid development of turbulent flow towards the inlet region and avoid flow recirculation on the outlet region.

3.2. Flow Parameters

3.2.1. Flow and heat transport

In order to mimic the core of an HTR realistically, flow is imposed via an inlet boundary condition at the top of the geometry, and a pressure outlet boundary at the bottom of the domain. Helium is considered as a working fluid with an imposed mass flow rate of 0.01607 kg/s. Based on the pebble diameter and the predicted maximum velocity, the estimated Reynolds number is 9753. The inlet temperature of helium is 773 K and constant properties at this temperature are used, as given in Table 1. The synthetic eddy method (SEM) [17] is used to generate and sustain the turbulence level at the inlet section. Periodic boundary conditions are imposed for mass flow and temperature on all four sides (i.e. in x- and z-directions) of the computational domain. The adopted configuration replicates the scenario of a very large pebble bed, as is the case for the core of a pebble bed reactor. It should be observed that in reality heat is produced by the nuclear fuel within the pebbles, while simultaneously being transported by conduction

within the pebble. Prediction of accurate temperature distribution for the reactor fuel will therefore require solving heat transport in both fluid and solid domain, including the conjugate heat transfer. However, the present work aims at simulating the cooling behavior accurately, and producing a reference database for a given heat input condition, rather than reproducing a realistic reactor temperature distribution. Therefore, it is limiting to adopt the simplifying assumption of an equivalent uniform heat flux of $8,317 \text{ W/m}^2$, applied on the pebble surfaces. All the flow parameters for this simulation are summarized in Table 1.

Table I. Flow parameters

Properties	Values	Units
Density	5.36	kg/m^3
Viscosity	$3.69 \cdot 10^{-5}$	N.s/m^2
Thermal Conductivity	0.3047	W/m.K
Specific Heat	5441.6	J/kg.K
Mass Flow Rate	0.01607	kg/s
Inlet Temperature	773	K
Heat Flux	8317	W/m^2
Prandtl number	0.66	-
Inlet Turbulence Level	25	%

3.2.2. Dust transport

For the validation cases of flow over a single sphere and an array of spheres, air is used as carrier fluid with density 1.205 kg/m^3 and viscosity of $1.821 \cdot 10^{-5} \text{ N.s/m}^2$. At the inlet, a velocity of 13.948 m/s with 5% turbulence intensity is applied. The Reynolds number based on the sphere diameter is 6000.

A particle density of 915 kg/m^3 is considered. Particles with a diameter range of 1 to $16 \mu\text{m}$ are injected from the domain inlet. The injection area is 3 times the sphere diameter with the center aligned with the center of the sphere(s) in the streamwise direction. In the case with a single sphere, about 30000 particles are injected in the projected area of the sphere for each particle diameter. In the case of an array of 8 spheres, about 90000 particles are injected in the projected area of the sphere for each particle diameter.

For the random pebble-bed arrangement study, Helium is considered as a working fluid. As described in the previous section, the LES simulation was done with a flow rate of 0.01607 kg/s . This corresponds to a maximum Reynolds number of 9752. In several inter-pebble gaps, the local Reynolds number could be much lower where phenomenon such as flow re-laminarization and transition to turbulence could occur. While an LES model is very much capable of resolving such complex phenomena, RANS turbulence models are more suitable for fully developed turbulent cases. In order to avoid flow complexities for RANS modeling, we have increased the mass flow rate by ten folds to 0.1607 kg/s . A turbulence intensity level of 5% is considered at the inlet. Wall boundary conditions are imposed on all four sides of the computational domain.

The particle density is equal to 912 kg/m^3 . Particles with a diameter range of 5 to $300 \mu\text{m}$ are injected with uniform distribution all over the inlet surface. About 80000 particles per particle diameter are injected from the inlet surface.

3.3. Computational Mesh

3.3.1. Flow and heat transport

Mesh generation for such a complex geometry is a particularly challenging task, and poses severe restrictions on the application structured meshing approaches. The commercially available STAR-CCM+ software allowed generating a fully polyhedral mesh inside the flow domain. This provides an optimal cell quality for the solution of the bulk flow, with the addition of boundary fitted prism cell layers in the near wall region, which is fundamental to accurately capture the high gradient near-wall flow. Figure 3 displays the generated polyhedral mesh, together with the boundary fitted layer near the pebble walls. This mesh consists of approximately 18 million grid cells, with a dimensionless mesh size lower than 1 in the wall normal direction, 10 in the azimuthal and 12 in the cross-sectional directions. The non-dimensional mesh size Δ^+ is defined as $\Delta u_\tau/\nu$; Δ =desired cell size, u_τ = friction velocity and ν = kinematic viscosity. The appropriateness of the adopted mesh quality has been thoroughly confirmed, and was presented in an earlier comparative study between LES and quasi-DNS for an idealized pebble bed [18]. The work indicated that non-dimensional mesh sizing of 10 and 23 in azimuthal and cross-sectional directions, respectively, is sufficient for a well-resolved LES solution. The results obtained corresponding to that mentioned mesh were found to be in good agreement with the reference q-DNS solution, with a maximum deviation of ~6% (for the RMS values). It is worth mentioning that these mesh dimensions denote the inter-pebble flow region, while the grid is further refined in the region of area contacts, as observable in Fig. 3. The computational mesh is instead coarsened in the outlet section, to avoid reverse flow effects, and acting as a buffer zone. Figure 3 displays the computed y^+ ($= yu_\tau/\nu$; u_τ = friction velocity and ν = kinematic viscosity) distribution over the pebbles. The y^+ values remain below 0.3 for most of the domain, and correspond to the low wall shear stress regions. For the high wall shear stress regions the value of y^+ reaches a maximum of 0.5 with an average value of 0.41 throughout the domain. The range of y^+ is therefore appropriate for wall resolved LES solution.

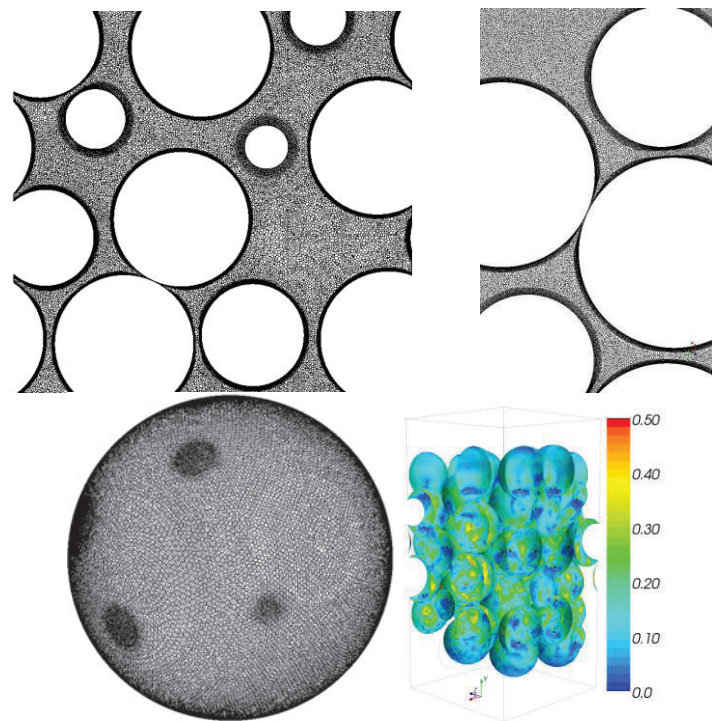


Figure 3. Polyhedral mesh across the computational domain in (top-left) front view, (top-right) zoom near the contacting pebbles and (bottom: left) on a single pebble and (bottom: right) the computed y^+ distribution over the pebbles.

3.3.2. Dust transport

A structured hexahedral mesh is used for the two validation cases of a single sphere and an array of spheres. A representation of the mesh over a single sphere is as shown in Fig. 4. A near-wall boundary layer of 12 cells is applied with clustering towards the wall. The first cell layer next to the wall has a $y^+ \sim 1$ with a stretching ratio of 1.2, which was sufficient to resolve the boundary layer.

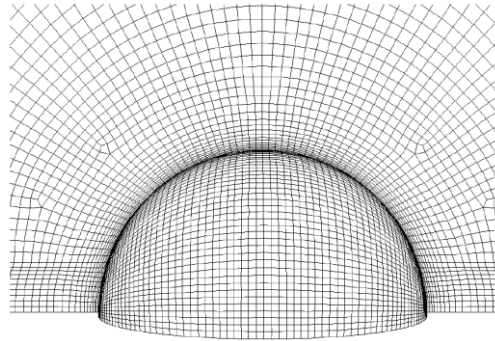


Figure 4. Structured Hexahedral mesh across a single sphere computational domain.

For the random pebble-bed, similar to the LES mesh as described in section 3.3.1, an unstructured polyhedral mesh is generated. The total mesh size is about 6.5 million cells. A near-wall boundary layer with approximately 7 cells are applied with clustering towards the wall. The first cell layer next to the wall had a $y^+ \sim 1$ with a stretching ratio of 1.2.

3.4. Turbulence Model

3.4.1. Flow and heat transport

The analyses are done through the CFD software Star-CCM+. Large eddy simulation (LES) is adopted as turbulence modeling approach for the flow and heat transport study. In LES, the large-scale motions are explicitly resolved, while the motion of small-scales, which is taking place below the limits of the numerical grid, are represented by a sub-grid model. The underlying premise is that the large three-dimensional eddies, which are dictated by the geometry and boundary conditions of the flow, are directly resolved, whereas the small eddies, which tend to be more isotropic, are modeled. In the present work, the wall-adapting local eddy-viscosity (WALE) model is selected.

3.4.2. Dust transport

The analyses are done through the CFD software ANSYS Fluent 14 because of the availability of a specially developed particle transport model in this code. The fluid phase is treated as incompressible. A pressure based solver in steady state conditions is applied. Turbulence is modeled through a standard $k-\epsilon$ model with enhanced wall treatment. Second order upwind scheme is selected for spatial discretization.

The particle transport modeling is based on the continuous random walk (CRW) model. Within this approach, the particle deposition modeling is divided into two regions namely, the boundary layer region where strong anisotropic turbulence prevails and bulk flow region where mainly isotropic turbulence is expected. The model is based on a Langevin equation. The Langevin equation takes different forms depending on the particle location which could be in the boundary layer or in the bulk region. For further details of the model formulation, please refer to [14].

4. RESULTS AND DISCUSSION

4.1. Flow and heat transport

Figure 5 displays an isometric view of the obtained numerical solution, highlighted by the instantaneous temperature distribution on the pebbles. The flow from top to bottom is depicted by the streamlines. At a first glimpse, the complexities appearing in the flow regime are evident. The pressure loss co-efficient across this limited sized random pebble bed is calculated to be 2.73.

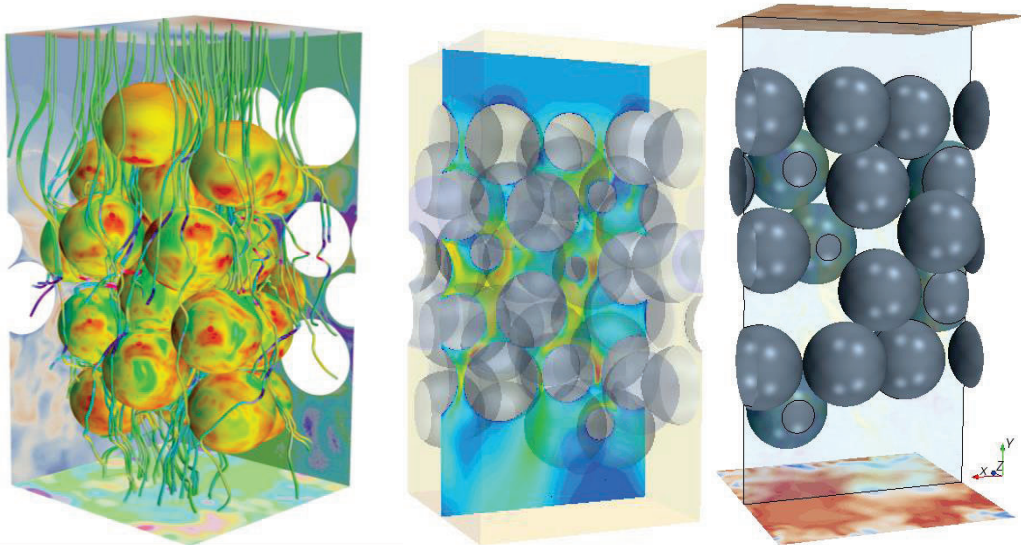


Figure 5. Isometric view of (left) the predicted flow features in the computational domain (middle) the selected z-plane along (right) with the pebbles connected to this plane.

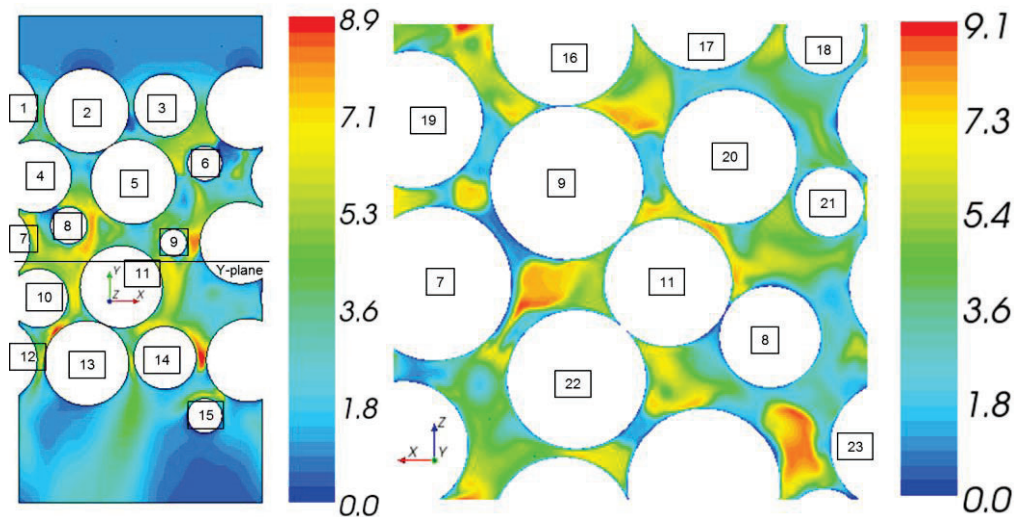


Figure 6. Iso-contours of time average velocity magnitude ($U^+ = U/U_{\text{inlet(ave)}}$) across (left) z- and (right) y-planes.

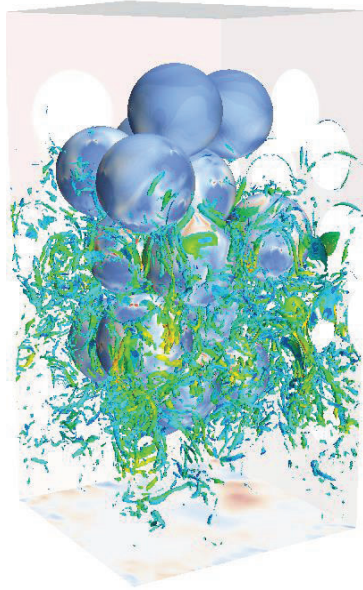


Figure 7. Iso-surfaces of Q-criterion ($Q=+5000$) colored by velocity magnitude.

In order to evaluate the flow distribution and its corresponding magnitude, a mid-section of the computational domain in the z -direction is selected and shown in Fig. 5. The selected z -plane contains a number of pebbles on either side, which drive the increased flow complexity evidenced by the mean velocity distribution in Fig. 6. The pebbles are identified by assigned numbers for clarity. The presented velocity is non-dimensionalized by the average inlet value. The iso-contours of mean velocity magnitude display a range of low and high velocity streaks, including stagnation regions and high velocity jets appearing in the narrow inter-pebble gaps. Moreover, sudden jumps appear in the velocity fields, such as near the pebbles 1-6-4, 4-8, 12-14, etc. A mid-section in the y -direction is also extracted, as given in Fig. 8, which also illustrates the appearance of high velocity magnitudes on the xz -plane. This suggests highly three-dimensional flow with strong rotational and stream curvatures. These complex flow features are also well depicted by the iso-surfaces of Q -criterion shown in Fig. 7. These iso-surfaces are extracted for a high positive value of Q (i.e. +5000), which represents regions of highly rotational flow.

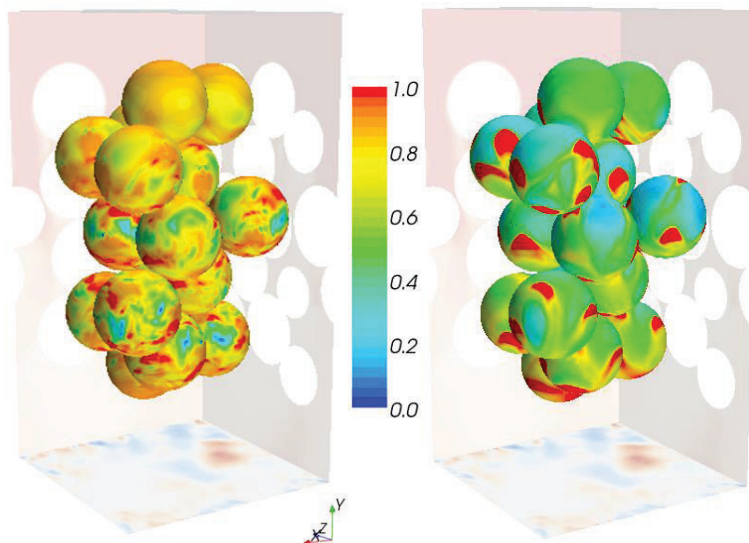


Figure 8. Iso-contours of (left) instantaneous and (right) time averaged temperature distribution over the pebbles; $T^+ = (T - T_{in}) / \Delta T_{conv}$.

Figure 8 displays the instantaneous temperature distribution over a selected set of pebbles appearing in the center of the computational domain. It is evident that all pebbles exhibit a wide range of temperatures. Further, several hot-spots appear, and correspond to previously discussed low velocity regions. These hot spots are also found to be unsteady, as consequence of the fast varying three dimensional flow. The time averaged temperature distribution of the pebbles surface is also displayed in Fig. 8. It should be noted here that, as previously discussed, an imposed heat flux is adopted for the simulation rather than the complete conjugate heat transfer solution. As a result of this simplification, peaks in the temperature prediction appear at the contact point locations, due to the absence of heat conduction through the solid pebbles. This also results in high local Nusselt numbers over the pebble surfaces. The heat transfer in terms of average Nusselt number for a subset of pebbles is calculated, i.e. pebble # 2, 3, 5, 11, 13 and 14 (as in Fig. 6) and is found to be 608.2, 607.4, 614.8, 616.2, 614.7, 615.3 respectively.

4.2. Dust transport

In this section the results of single sphere, array of spheres and the random pebble-bed simulations are presented. In each configuration, the resulting flow field is first discussed, followed by the results of particle deposition.

The flow fields around the single sphere are shown in Fig. 9. As seen in the velocity magnitude contour, the flow coming from upstream impinges on the sphere surface to form a stagnation zone in the front and the flow accelerates towards the top. After about 90 degrees, flow separation occurs and a big recirculation zone is formed behind the sphere. The maximum kinetic energy prevails in the wake region where high velocity gradients occur.

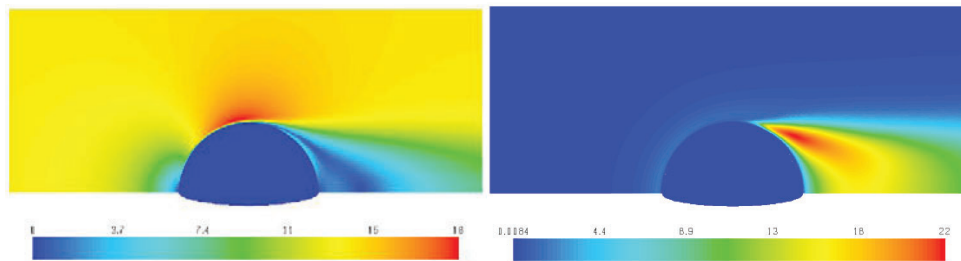


Figure 9. Flow over single sphere: Contours of (left) velocity magnitude and (right) turbulent kinetic energy.

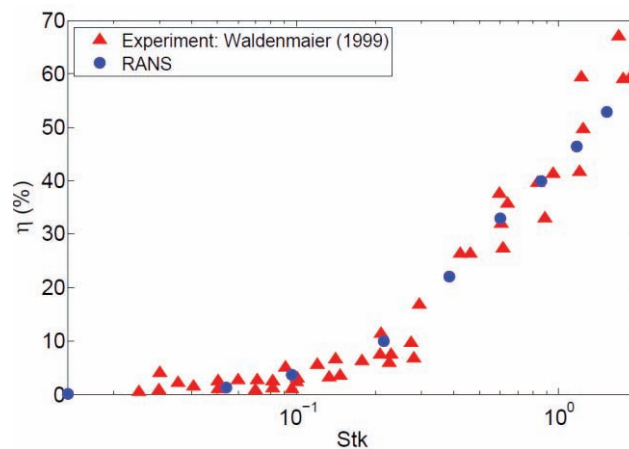


Figure 10. Deposition efficiency on a single sphere. Results of current simulation compared with the experimental data of [16].

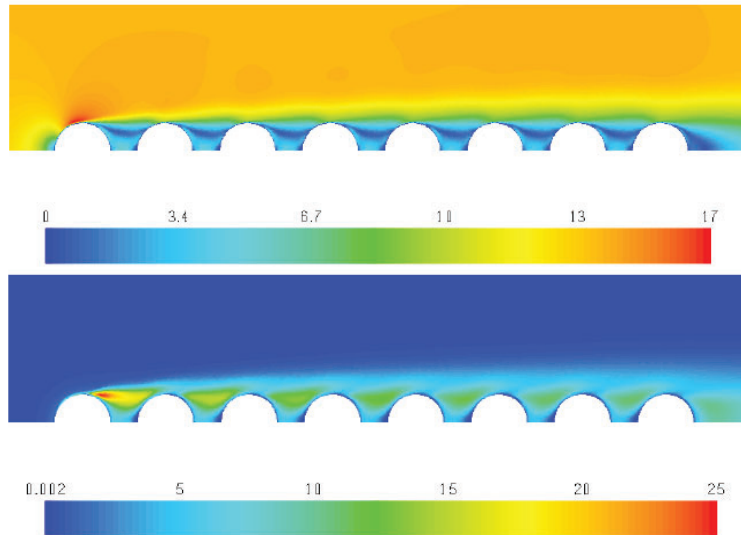


Figure 11. Flow over array of spheres: Contours of (left) velocity magnitude and (right) turbulent kinetic energy.

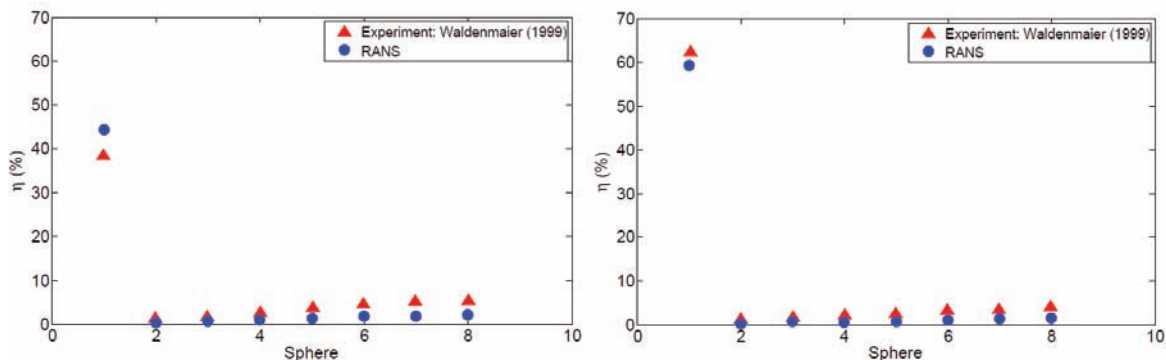


Figure 12. Deposition efficiency on an array of 8 sphere for (left) Stokes 1.2 and (right) Stokes 2.3. Results of current simulation compared with the experimental data of [16].

Figure 10 shows the deposition efficiency as a function of the particle Stokes number. The deposition efficiency is in good accordance with experimental results for a wide range of Stokes numbers.

The velocity magnitude and kinetic energy contours around an array of 8 spheres are shown in Fig. 11. Similar to the single sphere, the flow separation happens at the top of the first sphere. Because of the recirculation zone behind first sphere, most of the flow is directed towards the top surface of rest of the spheres. The recirculation zone prevails in the gaps between all spheres, as well as the last sphere. As expected, the kinetic energy is higher in the recirculation zones. The maximum value of kinetic energy is seen in the recirculation zone formed behind the first sphere and the intensity gradually decreases as we go further downstream.

Figure 12 shows the deposition efficiency for two Stokes numbers of 1.2 and 2.3 respectively. The highest value of deposition efficiency is on the first sphere of the array as the smooth flow upstream of the first sphere ensures maximum sphere area exposed to the incoming particles. The maximum difference in deposition prediction is on the first sphere which is about 5%. Compared to the first sphere, there is a significant drop in the deposition on rest of the spheres. The main reason is that less sphere area is exposed to the incoming flow due to the recirculation zones. The deposition trend of such a significant drop in deposition is captured reasonably well by the present dust transport model.

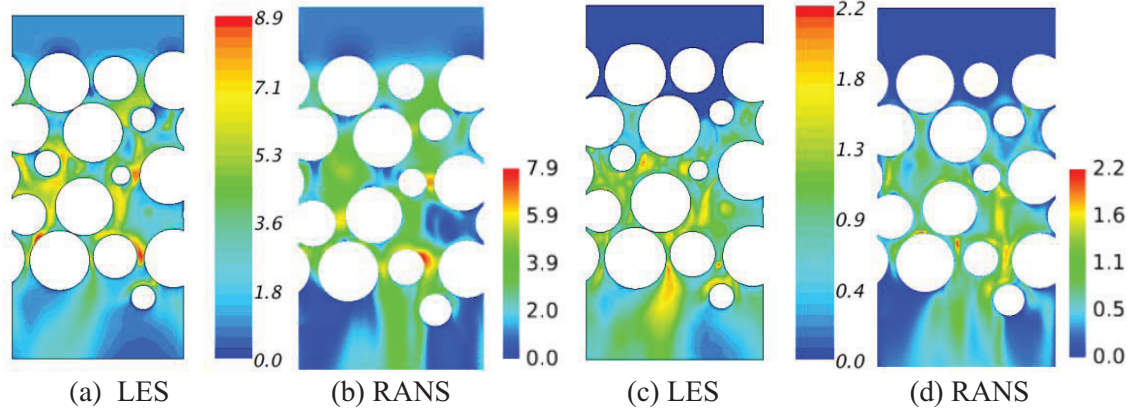


Figure 13. Iso-contours of (left) normalized velocity magnitude and (right) normalized flow kinetic energy across a plane in the flow direction.

The reasonably well predicted results for the dust deposition on a single sphere and an array of spheres forms basic validation of the particle solver chosen for this study. In the next part, this validated model is used to analyze the particle transport and deposition patterns in a randomly stacked pebble-bed arrangement.

In order to evaluate the flow distribution and its corresponding magnitude in the random pebble-bed RANS simulation, a mid-section of the computational domain in the flow direction is selected and shown in Fig. 13. For the sake of comparison, the LES results are shown next to the RANS results. The iso-contours of normalized mean velocity magnitude display a range of low and high velocity streaks, including stagnation regions and high velocity jets appearing in the narrow inter-pebble gaps. The regions of high and low velocity streaks are qualitatively comparable between RANS and LES. The kinetic energy is amplified soon after the flow moves downstream of the first set of pebbles. The amplification of kinetic energy is seen throughout the pebble-bed region and it also prevails downstream of the last set of pebbles. The regions of high and low kinetic energy are qualitatively comparable between RANS and LES.

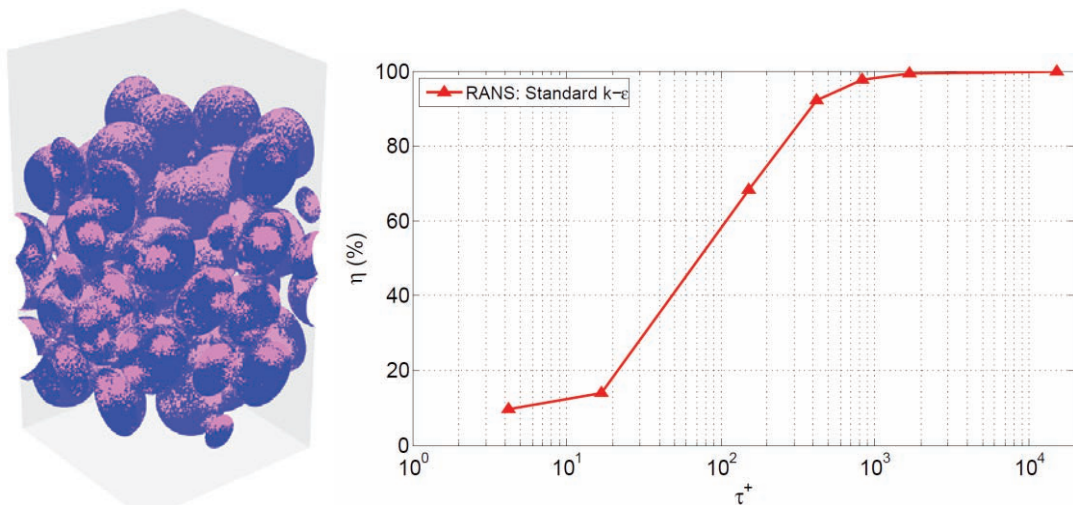


Figure 13. (left) Deposition patterns on the random pebble-bed surfaces for particle diameter of 100µm; (right) Deposition efficiency predictions in the considered random pebble-bed arrangement for a range of particle diameters.

The particle deposition patterns on the random pebble surfaces are as shown on the left of Fig. 14 for a particle diameter of 100 μm . In the first layer of spheres, the particle deposition is directly on the front surface which is facing the incoming particles. As the particles move through the domain, the deposition becomes random which is guided by the random and complex flow patterns prevailing in the inter-pebble regions.

The deposition efficiency for a range of particle diameters are as shown on the right of Fig. 14. The particles studied are in range 5-300 μm . Increase in particle diameter obviously increases the deposition efficiency due to increased inertial deposition.

5. SUMMARY AND CONCLUSIONS

Large eddy simulation was performed to analyze the flow and heat transport in a randomly stacked bed of spherical pebbles, using a second-order accurate, cell-centered finite volume method on an unstructured polyhedral mesh. The predicted flow-field was fairly complex and exhibits highly unsteady and three-dimensional turbulent behavior with strong rotational and cross flow regions. The reported high quality LES analyses results can be used for validation of low-order turbulence modeling applications to complex pebble flow configurations. Owing to high computational requirements for dust transport simulations using LES, the more practical RANS simulations of flow and dust transport were performed in a random pebble bed arrangement. The dust transport model was validated across two test cases of flow over single and array of spheres where reference experimental data were available. The validation results showed fairly accurate predictions of dust deposition for varied Stokes numbers. The maximum difference in deposition efficiency was found to be about 5%. The validated model was used to analyze the dust transport and deposition patterns in a randomly stacked pebble-bed arrangement. As expected, deposition becomes random which is guided by the complex flow patterns prevailing in the inter-pebble regions. The deposition fractions for varied particle diameters were analyzed.

ACKNOWLEDGEMENTS

The work described in this paper is funded by the Dutch Ministry of Economic Affairs, the FP7 EC Collaborative Project THINS No. 249337, and the FP7 EC Collaborative Project ARCHER No. 269892. These funding's are gratefully acknowledged.

REFERENCES

1. Groot, de S., Fütterer, M. A., Roelofs, F., Kohtz, N., Somers, J., Laurie, M., Buckthorpe, D., Scheuermann, W. 2013. The European (V)HTR R&D Project Archer: Overview, First Results And Outlook. Proceedings of ICAPP 2013, Jeju Island, Korea, April 14-18, Paper No. 206
2. Janse van Rensburg, J.J., Viljoen, C., van Staden, M.P., 2006. CDF modeling of high temperature gas cooled reactors. In: Proceedings of ICAPP'06, Reno, NV, USA, Paper 6304.
3. Janse van Rensburg, J.J., Kleingeld, M., 2011, August. An integral CFD approach for the thermal simulation of the PBMR Reactor Unit. Nucl. Eng. Des. 241 (8), 3130–3141.
4. IAEA. 2001. Current status and future development of modular high temperature gas cooled reactor technology, IAEA-TECDOC-1198.
5. Moormann R., A safety re-evaluation of the AVR pebble bed reactor operation and its consequences for future HTR concepts, Jül-4275, Jülich, Forschungszentrum, Germany.
6. Hassan Y. A., 2008, Large eddy simulation in pebble bed gas cooled core reactors, Nuclear Engineering and Design, vol. 238, pp. 530-537.

7. Kissane, M. P., 2009. A review of radionuclide behavior in the primary system of a VHTR. *Nuclear Engineering and Design* 239, 3076–3091.
8. Dominguez O. E. E., Perez C. E., Hassan Y. A., 2008, Measurements of flow modification by particle deposition inside a packed bed using time-resolved PIV, *Proceedings of 4th International Meeting on High Temperature Reactor technology HTR2008*, September 28 – October 1, Washington DC, USA.
9. Lee J. Y., Lee S. Y., 2008, Flow visualization of pebble bed HTGR, *Proceedings of the 4th International Meeting on High Temperature Reactor Technology HTR2008* September 28-October 1, 2008, Washington DC, USA.
10. Lee J. Y., Lee S. Y., 2010, Measurement of flow and thermal field in the pebble bed core of the VHTRG, *Proceedings of the 5th International Meeting on High Temperature Reactor Technology HTR2010* October 18-20, 2010, Prague, Czech Republic.
11. Smith, B. L., Mahaffy, J. H., Angele, K., Westin, J. 2011. Report on the OECD/NEA-Vattenfall T-junction Benchmark Exercise. NEA/CSNI/R(2011)5.
12. IAEA. 2010. Pressurized Thermal Shock in Nuclear Power Plants: Good Practices for Assessment. IAEA-TECDOC-1627.
13. Gosman, A., Ioannides, E., 1983. Aspects of computer simulation of liquid fuelled combustors. *Journal of Energy* 7, 482–490.
14. Jayaraju, S.T., Sathiah, P., Roelofs, F., Dehbi, A., 2015. RANS modeling for particle transport and deposition in turbulent duct flows: Near wall model uncertainties. *Nuclear Engineering and Design*, in-review.
15. Pavlidis, D., Lathouwers D., 2013, Realistic packed bed generation using small numbers of spheres, *Nuclear Engineering and Design*, Volume 263, October 2013, Pages 172–178.
16. Waldenmaier, M., 1999. Measurements of inertial deposition of aerosol particles in regular array of spheres. *Journal of Aerosol Science* 30, 1281–1290.
17. Jarrin, N., Benhamadouche, S., Laurence, D., Prosser, R., 2006. A synthetic-eddy method for generating inflow conditions for large-eddy simulations. *Int. J. Heat Fluid Flow* 27 (4), 585–593.
18. Shams, A., Roelofs, F., Komen, E.M.J., Baglietto, E., 2013. Large Eddy Simulation of a nuclear pebble bed configuration. *Nuclear Engineering and Design*, Vol. 261, August 2013, Pages 10–19.